Available online at www.sciencedirect.com
ScienceDirect
Journal of Sound and Vibration 306 (2007) 252–270
JOURNAL OF SOUND AND VIBRATION
www.elsevier.com/locate/jsvi

Vibration analysis of arbitrarily shaped membranes using local radial basis function-based differential quadrature method

W.X. Wu[a], C. Shu[a,*], C.M. Wang[b]

[a]*Department of Mechanical Engineering, National University of Singapore, 10 Kent Ridge Crescent, Singapore 117576, Singapore*
[b]*Engineering Science Programme and Department of Civil Engineering, National University of Singapore, 10 Kent Ridge Crescent, Singapore 117576, Singapore*

Received 26 April 2006; received in revised form 10 May 2007; accepted 12 May 2007
Available online 22 June 2007

Abstract

In this study, a recently developed local radial basis function-based differential quadrature (LRBFDQ) method is applied for the vibration analysis of arbitrarily shaped membranes. LRBFDQ method combines the good features of differential quadrature (DQ) approximation of derivatives and mesh-free nature of the radial basis functions (RBFs) in a local region. The derivative at a reference point is approximated as a linear weighted sum of functional values at a set of scattered points in the local supporting region of the reference point. The Helmholtz equation governing membrane vibration is directly discretized into algebraic equations, from which the wavenumbers (natural frequencies) and mode shapes of freely vibrating membranes are easily calculated. Owing to the properties of mesh-free and local approximation of the LRBFDQ method, the problems with arbitrarily shaped domains can be solved readily and accurately. In particular, for highly concave-shaped membranes and multi-connected membranes with a hole, very accurate numerical results can be easily obtained without the use of any domain decomposition technique. It is also shown that the LRBFDQ method can produce more accurate solutions than FEM when the two methods use nearly the same number of points in a domain.

1. Introduction

It is well known that there is an analogy between membrane vibration and plate vibration, i.e., the eigenvalues (natural frequencies) of a simply supported polygonal plate are the squares of the eigenvalues (wavenumbers) of a membrane under constant tension with identical geometry and fixed edges, and their eigenfunctions (mode shapes) are identical [1–8]. This analogy has greatly evoked researchers' interest in vibration analysis of membranes because the solutions for polygonal membranes can be converted into those of polygonal simply supported plates. For a membrane of a simple geometry such as rectangle, circle or ellipse, exact solutions for the transverse vibration are available [9–11]. However, for a membrane of a complex geometry, only numerical solutions may be possible. Conway and Farnham [1] used special adaptations of the

*Corresponding author. Tel.: +65 68746476; fax: +65 67791459.
E-mail address: mpeshuc@nus.edu.sg (C. Shu).

0022-460X/$ - see front matter © 2007 Elsevier Ltd. All rights reserved.
doi:10.1016/j.jsv.2007.05.015

point-matching method to determine the numerical solutions for the fundamental wavenumbers of isosceles triangular, rhombic and parallelogram membranes, which were converted from the plate results based on the aforementioned analogy. Durvasula [2] used the Rayleigh–Ritz method, with the deflection expressed as a double Fourier sine series in oblique coordinates, to obtain the first several wavenumbers and mode shapes of a wide range of skew membranes. Bauer and Reiss [3] employed an iterative procedure, in which a finite difference method (FDM) with a triangular mesh was used, to obtain twenty-eight wavenumbers and mode shapes of 60° rhombic membranes. Irie et al. [4,5] used a series-type solution, in which a polygonal membrane was formed on a rectangular membrane by fixing several segments, to calculate the wavenumbers and mode shapes of regular polygonal membranes and concavely shaped polygonal membranes. More recently, Kang et al. [7,8] used the non-dimensional dynamic influence function and the finite element software of ANSYS to obtain wavenumbers and mode shapes for some convex-shaped membranes with single domains. They also used the same method together with the domain decomposition technique to obtain wavenumbers of highly concave-shaped membranes and multi-connected membranes with a hole.

In the aforementioned studies, all the numerical methods rely on a mesh which is formed from a series of points with a specific element or mesh structure. To maintain detailed structural information about the computational mesh, comprising all nodal and element-based connectivity and hierarchical data, is very expensive and tough. To overcome these difficulties, it is highly desirable to have a numerical method which only uses the information at points, and in the meantime, can obtain accurate numerical results for problems with arbitrary domain shapes. As a part of the effort in this research direction, Shu et al. [12] recently developed a local radial basis function-based differential quadrature (LRBFDQ) method, which could be applied to solve membrane problems with complex geometry.

In the development of the LRBFDQ method, the concept of differential quadrature (DQ) was adopted. DQ method was proposed by Bellman et al. [13] in 1972. Its basic idea is that the derivative at a mesh point along a mesh line is approximated by a linear weighted sum of the functional values at all the mesh points along the mesh line. DQ is a global method, which can obtain accurate numerical results by using a considerably small number of mesh points. So far, DQ method has been efficiently applied to solve many engineering problems [14–22]. It should be indicated that the conventional DQ method is based on one-dimensional polynomial approximation, which can only be applied along a straight mesh line. This greatly limits its application to problems with curved boundary. The LRBFDQ method was developed to remove such a limitation. In the LRBFDQ method, the RBFs are taken as the base functions in a local region, which can be collocated at neighboring points randomly distributed around a reference point, and DQ formulation is used to approximate derivative at the reference point. Obviously, LRBFDQ method combines the mesh-free nature of RBFs and derivative approximation of DQ method. Due to this feature, it can be easily applied to problems with complex geometry. For any problem, the derivative at a reference point is approximated by LRBFDQ in the form of a weighted linear sum of functional values at a set of scattered points in the local supporting region of this reference point. So far, LRBFDQ method has been efficiently applied to solve fluid flow problems [12].

In this study, LRBFDQ method is applied for vibration analysis of arbitrarily shaped membranes to further demonstrate its high accuracy and efficiency. After numerical discretization by LRBFDQ method, Helmholtz equation, which governs the vibration of membranes, will be reduced to an algebraic equation. By collocating the discrete algebraic equation at all interior points, which are scattered, a system of algebraic equations will be obtained. This system is well posed after implementation of the boundary condition. Wavenumbers and mode shapes of membranes can be readily obtained by solving this system of equations. Owing to the properties of mesh-free and local approximation of the LRBFDQ method, it is shown in this paper that the membrane problems with arbitrarily shaped domains such as highly concave-shaped membranes and multi-connected membranes with a hole can be accurately and efficiently solved without using any domain decomposition technique.

This paper is organized as follows: Section 2 gives an introduction for the vibration analysis of arbitrarily shaped membranes by using LRBFDQ method. Section 3 defines the vibration problem of membrane and shows the solution procedure of the LRBFDQ method. Section 4 discusses the determination of the shape parameter c in the chosen RBF. Section 5 presents numerical results and discussion. Finally, the conclusions of this study are given in Section 6.

2. Local radial basis function-based differential quadrature (LRBFDQ) method

2.1. Radial basis functions

A radial basis function (RBF), denoted by $\varphi(\|\mathbf{x}-\mathbf{x}_j\|_2)$, is a continuous real-valued function defined on $[0, \infty)$ and it depends on the distance $r(\mathbf{x}, \mathbf{x}_j) = \|\mathbf{x}-\mathbf{x}_j\|_2$ between two points $\mathbf{x}$ and $\mathbf{x}_j$ in a problem domain Ω which is in the space $\mathbf{R}^d$, i.e. $\mathbf{x}, \mathbf{x}_j \in \Omega \subset \mathbf{R}^d$, where $d = 1$, 2 or 3 denotes the dimension of the space. There are many forms of RBF, but in this study, we will only use the inverse quadratics (IQs) expressed by

$$\varphi(r) = \frac{1}{r^2 + c}, \quad c > 0, \tag{1}$$

where c is the shape parameter.

2.2. Global RBF-based interpolation method

Assume that a finite physical quantity, F, is piecewise continuous in a finite domain, Ω. F is known only at a finite number of locations, $\{\mathbf{x}_j : j = 1, 2, \ldots, N\}$, where $\mathbf{x}_j = x_j$ for a univariate problem, and $\mathbf{x}_j = (x_j, y_j, \ldots)^{\mathrm{T}}$ for a multivariate problem. From the finite amount of information regarding F, we seek the best approximation which not only supplies accurate estimates of F at arbitrary locations on the domain, but it will also provide accurate estimates of the partial derivatives and definite integrals of F anywhere on the domain. Consider an interpolation function, f, which approximates F in the sense that

$$f(\mathbf{x}_j) = F(\mathbf{x}_j), \quad j = 1, 2, \ldots, N. \tag{2}$$

Then at an arbitrary location $\mathbf{x}$ on the domain, the interpolation function $f(\mathbf{x})$ can be written as a linear combination of N radial basis functions and a polynomial of order not exceeding q,

$$f(\mathbf{x}) = \sum_{j=1}^{N} \lambda_j \varphi\left(\left\|\mathbf{x}-\mathbf{x}_j\right\|_2\right) + \sum_{k=1}^{n} \varsigma_k P_k(\mathbf{x}), \tag{3}$$

where $n = (q+d)!/(q!d!)$. From Eq. (2), we obtain the following equation system:

$$\sum_{j=1}^{N} \lambda_j \varphi\left(\left\|\mathbf{x}_i-\mathbf{x}_j\right\|_2\right) + \sum_{k=1}^{n} \varsigma_k P_k(\mathbf{x}_i) = F(\mathbf{x}_i), \quad i = 1, 2, \ldots, N. \tag{4}$$

Equation system (4) has N equations with $N+n$ unknowns $\lambda_j, j = 1, 2, \ldots, N$, $\varsigma_k, k = 1, 2, \ldots, n$. Obviously, it is not a well-posed problem. To solve this equation system, we need n auxiliary equations. According to the work of Kansa [23,24], the auxiliary equations can be given by

$$\sum_{j=1}^{N} \lambda_j P_k(\mathbf{x}_j) = 0, \quad k = 1, \ldots, n. \tag{5}$$

2.3. Differential quadrature method

When the global interpolation is replaced by local interpolation, and the concept of DQ method is introduced, the global RBF-based interpolation method can be modified into the LRBFDQ method. The DQ method is a numerical discretization technique to approximate derivatives [13]. It was initiated from the idea of integral quadrature. The essence of the DQ method is that the partial derivative of a function at a reference point can be approximated by a weighted sum of the functional values at all discrete points within the supporting region of this reference point. Referring to Fig. 1, where an unstructured distribution of points in a problem domain is shown, the index i represents a reference point and ij ($j = 1, \ldots, m$) a group of points in the local supporting region of the

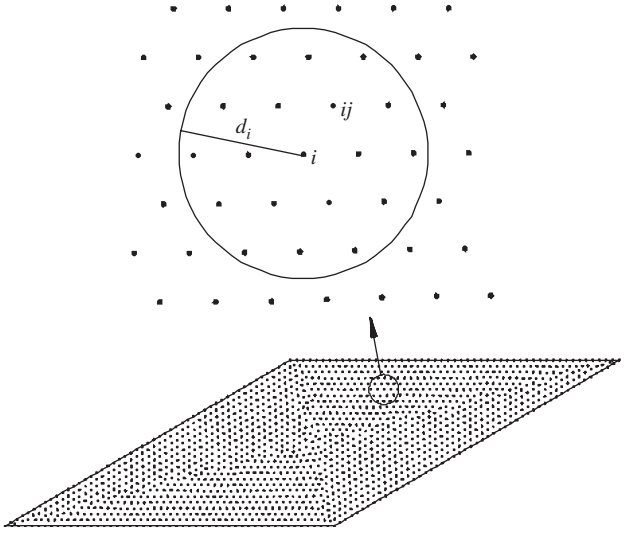

Fig. 1. A computational domain with an unstructured distribution of points.

point i. For any continuous and differentiable function $f(\mathbf{x})$, we have, for example,

$$\frac{\partial f_i}{\partial x} = \sum_{j=1}^{m} T_{i,j}^{(1x)} f_{ij} + T_{i,m+1}^{(1x)} f_i, \tag{6}$$

where f_i and f_{ij} are the function values at the points $\mathbf{x}_i$ and $\mathbf{x}_{ij}$, respectively; and for simplicity, $\partial f_i/\partial x$ is used to represent the value of $\partial f/\partial x$ at the point $\mathbf{x}_i$. The key procedure in the DQ method is the determination of the weighting coefficients, $T_{i,j}^{(1x)}$ for the particular case in Eq. (6). It has been shown by Shu [14] that the weighting coefficients can be easily computed under the analysis of a linear vector space and the analysis of a function approximation.

2.4. LRBFDQ method

In the LRBFDQ method, RBFs are used as base functions to approximate the unknown function $f(\mathbf{x})$ only locally in the supporting region of the point $\mathbf{x}_i$ and only a constant is used as the polynomial term. Then, from Eq. (3), we have

$$f(\mathbf{x}) = \sum_{j=1}^{m} \lambda_j^i \varphi\left(\left\|\mathbf{x} - \mathbf{x}_{ij}\right\|_2\right) + \lambda_{m+1}^i \varphi(\|\mathbf{x} - \mathbf{x}_i\|_2) + \varsigma_1^i. \tag{7}$$

The coefficients λ_j^i $(j = 1, \ldots, m+1)$ and ς_1^i are associated with the supporting region of the point $\mathbf{x}_i$ and may be calculated by collocating Eq. (7) at the points $\mathbf{x}_i$ and $\mathbf{x}_{ij}$ $(j = 1, \ldots, m)$ with the auxiliary condition which is a modification of Eq. (5), i.e.,

$$\sum_{j=1}^{m+1} \lambda_j^i = 0 \Rightarrow \lambda_{m+1}^i = -\sum_{j=1}^{m} \lambda_j^i. \tag{8}$$

It is noted that the coefficients λ_j^i $(j = 1, \ldots, m+1)$ and ς_1^i are not necessary to be calculated in the framework of the LRBFDQ method.

Substitution of Eq. (8) into Eq. (7) yields

$$f(\mathbf{x}) = \sum_{j=1}^{m} \lambda_j^i g_j^i(\mathbf{x}) + \varsigma_1^i, \tag{9}$$

where

$$g_j^i(\mathbf{x}) = \varphi\left(\left\|\mathbf{x}-\mathbf{x}_{ij}\right\|_2\right) - \varphi(\|\mathbf{x}-\mathbf{x}_i\|_2), \quad j = 1, \ldots, m. \tag{10}$$

It can be seen from Eq. (9) that $f(\mathbf{x})$ constitutes an $(m+1)$-dimensional linear vector (function) space $\mathbf{V}^{m+1}$ with respect to operations of vector addition and scalar multiplication, and $g_j^i(\mathbf{x})$ $(j = 1, \ldots, m)$ and $g_{m+1}^i(\mathbf{x}) = 1$ form a set of base vectors in $\mathbf{V}^{m+1}$. According to the property of a linear vector space, any vector in the space can be uniquely expressed by a linear sum of all the base vectors. Another important property of a linear vector space is that if all the base vectors satisfy a linear relationship like Eq. (6), so does any vector in the space, which could be expressed by Eq. (9). This property guarantees that with the help of linear Eq. (6), the weighting coefficients $T_{i,j}^{(1x)}$ $(j = 1, \ldots, m+1)$ computed from the base vectors can be used to discretize the derivative of function $f(\mathbf{x})$, which could be the solution of a PDE and approximated by Eq. (9). By substituting all the base vectors, $g_j^i(\mathbf{x})$ $(j = 1, \ldots, m+1)$, into Eq. (6), one obtains

$$\frac{\partial g_j^i(\mathbf{x}_i)}{\partial x} = \sum_{k=1}^{m} T_{i,k}^{(1x)} g_j^i(\mathbf{x}_{ik}) + T_{i,m+1}^{(1x)} g_j^i(\mathbf{x}_i), \quad j = 1, \ldots, m, \tag{11a}$$

$$0 = \sum_{k=1}^{m} T_{i,k}^{(1x)} + T_{i,m+1}^{(1x)}. \tag{11b}$$

The $m+1$ weighting coefficients for a point $\mathbf{x}_i$, $T_{i,j}^{(1x)}$ $(j = 1, \ldots, m+1)$, can be determined by solving the $m+1$ Eqs. (11a) and (11b) since the values of these base functions and their derivatives at given points are readily known. The weighting coefficients for other derivatives can be obtained by using a similar process. Using these weighting coefficients, we can discretize spatial derivatives and transform a PDE into a system of algebraic equations, which can then be solved by iterative or direct methods. An important property of the LRBFDQ method is that it is naturally mesh-free, and only the information of positions of the scattered points in the domain is needed for discretization of derivatives.

3. Free vibration of uniform membranes

3.1. Definition of the problem

Consider the problem of transverse free vibration of a pre-stretched uniform membrane having no deflection at its edges. The governing differential equation is

$$\nabla^2 W + \Lambda^2 W = 0, \tag{12}$$

where $\nabla^2 = \partial^2/\partial x^2 + \partial^2/\partial y^2$ is the Laplacian operator, $W = W(x, y)$ is the modal transverse deflection, $\Lambda = \omega\sqrt{\rho/T}$ is the wavenumber, ρ is the mass per unit area, ω is the circular frequency, and T is the uniform tension per unit length. The boundary condition is

$$W = 0, \quad \text{on the edge } \Gamma. \tag{13}$$

The purpose of this study is to apply the LRBFDQ method with IQ as the RBF to solve Eq. (12) together with the boundary condition (13) for accurate wavenumbers and mode shapes of the arbitrarily shaped membranes. The validity and efficiency of the LRBFDQ method are illustrated through this study.

3.2. Numerical discretization by LRBFDQ

Before discretizing the governing differential equation, a preparation for some data is needed. At first, we need to generate a total of N unstructured nodal points (x_i, y_i), $i = 1, 2, \ldots, N$ in the domain Ω; the points with the global indices $i = 1, 2, \ldots, N_i$ are interior points, and the points with the global indices $i = N_i + 1, N_i + 2, \ldots, N$ are boundary points. Then, we generate a data file in which the global indices of m nearest supporting points around each point i $(i = 1, 2, \ldots, N)$ are given as ij $(j = 1, 2, \ldots, m)$. Finally, the weighting coefficients, $T_{i,j}^{(\nabla^2)}$ $(i = 1, 2, \ldots, N; j = 1, 2, \ldots, m+1)$, are calculated by using the procedure given in Section 2.4.

With availability of above data, Eq. (12) can be discretized at each interior point as

$$\sum_{j=1}^{m} T_{i,j}^{(\nabla^2)} W_{ij} + T_{i,m+1}^{(\nabla^2)} W_i = -\Lambda^2 W_i \quad \text{for } i = 1, 2, \ldots, N_i. \tag{14}$$

In the system (14), there are N_i equations in which W_i $(i = 1, 2, \ldots, N_i)$ and W_{ij} $(1 \leqslant ij \leqslant N)$ are unknowns. So there are N unknowns. By substituting the boundary conditions

$$W_i = 0 \quad \text{for } i = N_i + 1, N_i + 2, \ldots, N \tag{15}$$

into the system (14), the number of unknowns can be reduced to N_i which is equal to the number of equations. System (14) can then be written as a matrix–vector form

$$\mathbf{A}\mathbf{a} = -\Lambda^2 \mathbf{a}, \tag{16}$$

where the coefficient matrix $\mathbf{A} \in R^{N_i \times N_i}$, the vector $\mathbf{a} = [W_1, W_2, \ldots, W_{N_i}]^{\mathrm{T}}$. The wavenumbers Λ and the mode shapes given by the vector $\mathbf{a}$ of a vibrating membrane can be obtained by calculating the eigenvalues and eigenvectors of the matrix $\mathbf{A}$. In this study, the eigenvalues of matrices are computed by using HBG and HQR solvers [25], and the eigenvectors are computed by using a subroutine written by the authors.

4. Numerical test for determination of shape parameter c

By using the LRBFDQ method to solve a PDE, the factors that influence the accuracy and stability of numerical solutions may include the RBF used, the PDE to be solved, the boundary condition, the shape of domain, the density of the scattered points in the domain, the number of supporting points of each reference point, and the value of shape parameter c chosen. It could be a daunting task to clarify these influences. Even the research on an appropriate choice of c-value is still far from perfection, and there is hitherto no theoretical analysis on this topic. In this study, for the purpose of finding appropriate c-values for the vibrating membranes, we shall use IQ as the RBF in the LRBFDQ method to solve a sample Poisson equation, where the solution is guessed to be similar to the mode shapes of vibrating membranes.

Consider the two-dimensional Poisson equation in a square domain Ω $(0 \leqslant x \leqslant 1,\ 0 \leqslant y \leqslant 1)$,

$$\nabla^2 u = g(x, y). \tag{17}$$

Suppose that the exact solution is given as

$$u(x, y) = \frac{\frac{5}{4} + \cos(5.4y)}{6 + 6(3x - 1)^2}. \tag{18}$$

Eq. (18) is used to provide the Dirichlet condition on the boundary, the function $g(x, y)$, and to validate the numerical solution. This problem is analyzed by employing three random distributions of points with different spacings to study the convergence behavior of the method. The total numbers of points for the three distributions are $N = 488$, 1004 and 1531, respectively. The accuracy of the numerical results is assessed using the average L_2 norm of the relative error:

$$R_{L2} = \sqrt{\frac{1}{N} \sum_{i=1}^{N} \left(\frac{u_{\text{numerical}} - u_{\text{analytical}}}{u_{\text{analytical}}} \right)^2}. \tag{19}$$

Figs. 2–7 show $\mathrm{Log}_{10}(R_{L2})$ vs. c for different values of m. From Fig. 2 ($m = 10$), we observe that:

(1) the curves of error vs. the shape parameter c are very smooth. This implies that the numerical solutions are very stable when only 10 supporting points for each reference point are used;
(2) when the total number of scattered points in the domain increases, the accuracy of solution increases;
(3) for each distribution of the scattered points, there is an optimal value of c corresponding to the lowest error of solution, and the error increases along with the c-value varying away from this optimal value at both sides;

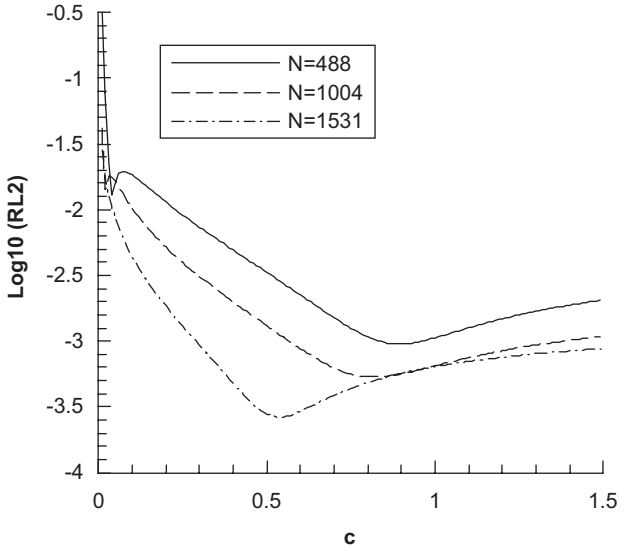

Fig. 2. $\mathrm{Log}_{10}(R_{L2})$ vs. c ($m = 10$).

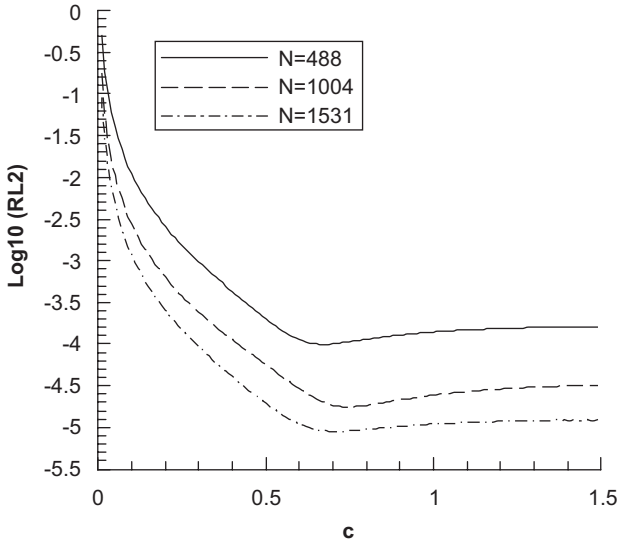

Fig. 3. $\mathrm{Log}_{10}(R_{L2})$ vs. c ($m = 16$).

(4) the optimal c-values for these three point distributions are located in a narrow region, which is found to be about $(0.5, 0.9)$ as shown in Fig. 2.

Fig. 3 shows $\mathrm{Log}_{10}(R_{L2})$ vs. c for $m = 16$ and indicates that:

(1) the numerical solutions are still very stable for the three point distributions;
(2) for each point distribution, the accuracy of solution increases substantially as compared to Fig. 2;
(3) the accuracy of solutions as shown in Fig. 3 (i.e. $-5 < \mathrm{Log}_{10}(R_{L2}) < -4$) is very satisfactory for solving a PDE;
(4) a large part of each curve is quite flat and almost parallel to the c-axis. This implies that the accuracy of solution is less affected by the c-value when c becomes larger than its optimal value;
(5) the region in which the optimal c-values are located becomes narrower, which is about $(0.6, 0.8)$.

Findings (1)–(3) show that the scheme with $m = 16$ can yield stable solutions with satisfactory accuracy for all the three point distributions. The last two findings are also very important because they facilitate a wide choice of appropriate c-values.

Fig. 4 shows the numerical error when $m = 22$. The solution is stable for the point distribution $N = 488$. But the range of c-values, allowing stable solution for the point distribution $N = 1004$, becomes very narrow, i.e., (0.6, 1.1). This narrow range makes the proper choice of c-values very difficult before carrying out this numerical test. In practice, when the analytical solution of a PDE is not known, it is very difficult to choose a good c-value if its range is so small and the location of this range is not known. For the point distribution $N = 1531$, the range of good c-values becomes even smaller, and the numerical solution becomes unstable immediately after the optimal c-value.

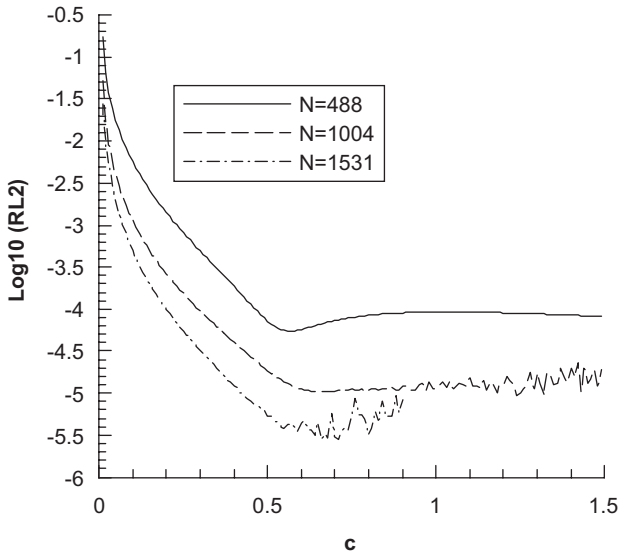

Fig. 4. $\mathrm{Log}_{10}(R_{L2})$ vs. c ($m = 22$).

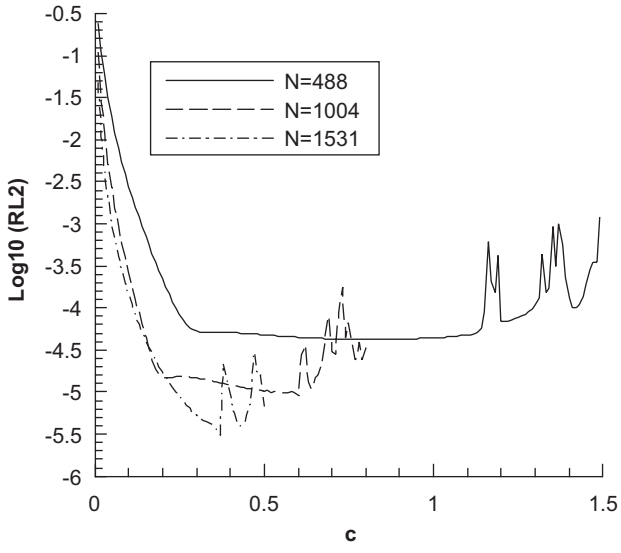

Fig. 5. $\mathrm{Log}_{10}(R_{L2})$ vs. c ($m = 28$).

As shown in Figs. 5–7 ($m \geqslant 28$), the ranges of c-values allowing stable numerical solutions for the point distribution $N = 488$ also become very small, and the solutions for $N = 1004$ and 1531 are extremely unstable. Therefore, we can conclude that the schemes with $m \geqslant 28$ are not suitable for solving this class of PDE when $N \geqslant 488$. From above investigation, it seems that the scheme with $m = 16$ and $0.6 \leqslant c \leqslant 1.5$ is the best choice for solving the sample PDE.

5. Results and discussion

The LRBFDQ method will be validated by its application to free vibration analyses of a number of membranes with various shapes. Firstly, the LRBFDQ results for circular and rectangular membranes are computed and compared with exact solutions [7], numerical solutions obtained by Kang et al. [7] using the

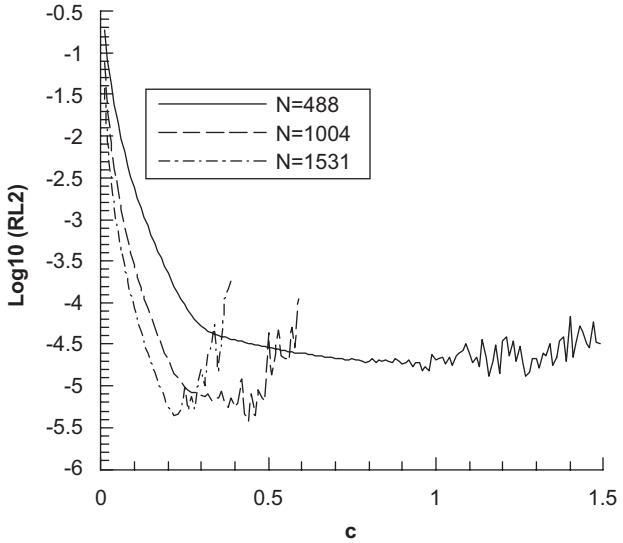

Fig. 6. $\mathrm{Log}_{10}(R_{L2})$ vs. c ($m = 36$).

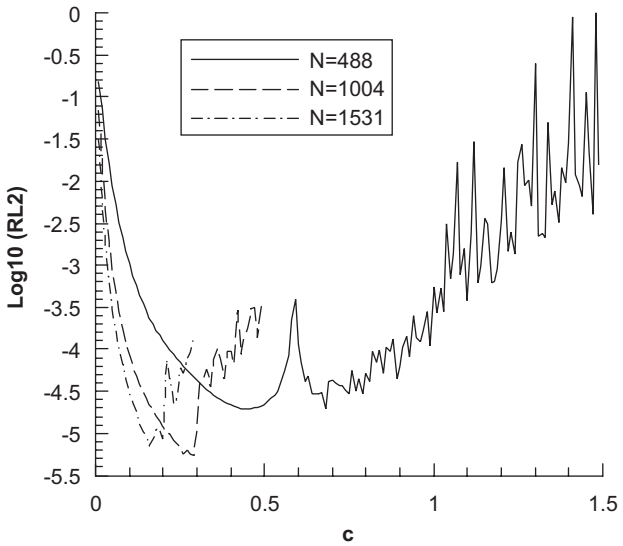

Fig. 7. $\mathrm{Log}_{10}(R_{L2})$ vs. c ($m = 46$).

non-dimensional dynamic influence function, and FEM solutions [7]. Next, the LRBFDQ method is applied to compute the wavenumbers and mode shapes for membranes with other complex shapes, and the results are compared with data of Kang et al. [8]. Note that all the FEM results were given by Kang et al. [7,8] using a commercial software of ANSYS. For all the cases, the LRBFDQ scheme with IQ as the RBF, $m = 16$ as the number of supporting points of each reference point, and $c = 1.0$ as the value of shape parameter is used.

5.1. Circular membrane

For the circular membrane of unit radius, three random distributions of points, i.e. $N = 629$, 1068, and 1490 are adopted to compute the first eight wavenumbers by using the LRBFDQ method. In Table 1, the LRBFDQ results are compared with the exact solutions [7], the numerical solutions obtained by Kang et al. [7] who used the non-dimensional dynamic influence function and 16 boundary points, and FEM results [7]. It can be seen that the LRBFDQ results in case of $N = 629$ are already very close to the exact solutions, and when the number of points in the domain increases, such as $N = 1068$ and 1490, the accuracy of the LRBFDQ results improves further. When $N = 1490$, all the LRBFDQ results are extremely accurate. As a comparison, we see that Kang's numerical results are also extremely accurate except that the error of Λ_7 is slightly large. When we compare the results obtained using LRBFDQ and the number of points $N = 1068$ with FEM results using nearly the same number of points ($N = 1024$), we find that the accuracy of LRBFDQ results is much better than that of FEM results.

The LRBFDQ method is further validated by computing the mode shapes of the membranes. The mode shapes of the first six modes of the circular membrane are plotted in Fig. 8, where the number of nodal diameters is denoted by n and the number of nodal circles is denoted by s, which does not include the boundary. According to the sequence of increasing values of wavenumbers, the first six vibrating modes of the circular membrane correspond to the pairs of n and s values as $(n = 0, s = 0)$, $(n = 1, s = 0)$, $(n = 2, s = 0)$, $(n = 0, s = 1)$, $(n = 3, s = 0)$ and $(n = 1, s = 1)$. We can also see that all the mode shapes are very smooth. Note that if accurate numerical results for wavenumbers cannot be obtained by using a certain method, it is certain that the mode shapes will not be smooth at some locations. Therefore, by observing these mode shapes, researchers can better understand why and where the numerical errors occur, and take appropriate measures to improve their numerical approach for better solutions.

5.2. Rectangular membrane

Next, we consider the free vibration of a rectangular membrane of size 1.2×0.9 which has exact solutions. The LRBFDQ results for the wavenumbers of the first eight modes are computed using three distributions of points in the membrane domain, i.e., $N = 530$, 1057 and 1503. Table 2 compares these results with the exact solutions [7], the numerical solutions obtained by Kang et al. [7] who employed the non-dimensional dynamic influence function and 24 boundary points, and the FEM results. It is found that the LRBFDQ results are in

Table 1
Comparison of wavenumbers of the circular membrane ($R = 1$) obtained by the present method, the analytical method [7], Kang et al. [7], and FEM [7]

Wavenumbers	LRBFDQ results			Exact solution [7]	Kang [7]	FEM, $N = 1024$ [7]
	$N = 629$	$N = 1068$	$N = 1490$			
Λ_1	2.4043	2.4046	2.4047	2.4048	2.4048	2.4166
Λ_2	3.8313	3.8315	3.8316	3.8317	3.8317	3.8513
Λ_3	5.1353	5.1355	5.1356	5.1356	5.1356	5.1744
Λ_4	5.5206	5.5203	5.5202	5.5201	5.5201	5.5515
Λ_5	6.3800	6.3801	6.3802	6.3802	6.3802	6.4610
Λ_6	7.0163	7.0160	7.0158	7.0156	7.0156	7.0592
Λ_7	7.5879	7.5883	7.5884	7.5883	7.5876	7.7445
Λ_8	8.4171	8.4175	8.4174	8.4172	8.4172	8.4841

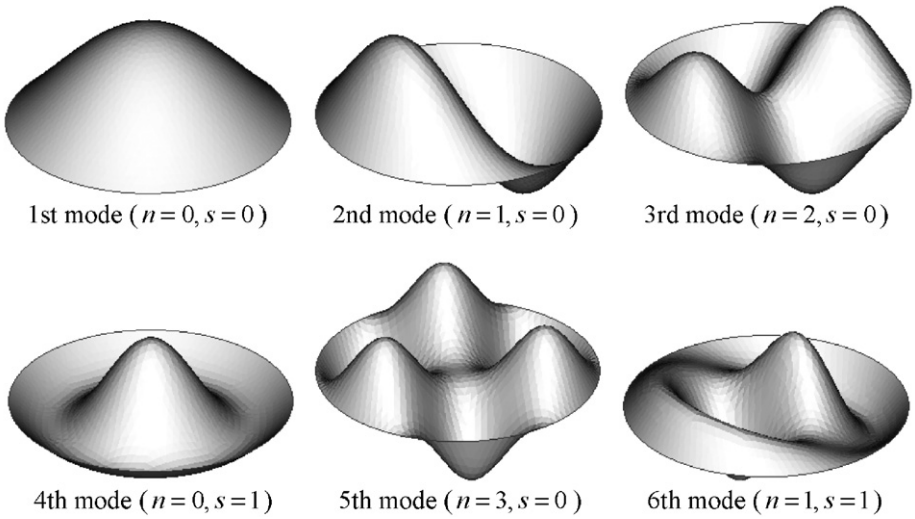

Fig. 8. Mode shapes of the circular membrane.

Table 2
Comparison of wavenumbers of the rectangular membrane (1.2×0.9) obtained by the present method, the analytical method [7], Kang et al. [7], and FEM [7]

Wavenumbers	LRBFDQ results			Exact solution [7]	Kang [7]	FEM, $N = 1089$ [7]
	$N = 530$	$N = 1057$	$N = 1503$			
Λ_1	4.3633	4.3633	4.3633	4.3633	4.3633	4.3651
Λ_2	6.2930	6.2929	6.2929	6.2929	6.2929	6.3006
Λ_3	7.4561	7.4561	7.4561	7.4560	7.4560	7.4669
Λ_4	8.5947	8.5948	8.5948	8.5947	8.5948	8.6213
Λ_5	8.7269	8.7267	8.7267	8.7266	8.7266	8.7407
Λ_6	10.5081	10.5082	10.5083	10.5083	10.5083	10.5370
Λ_7	10.7917	10.7938	10.7941	10.7943	10.7943	10.8313
Λ_8	11.0369	11.0381	11.0383	11.0384	11.0389	11.1029

very good agreement with the exact solutions and Kang's numerical results, and the accuracy of the LRBFDQ results is clearly much higher than that of the FEM results.

Fig. 9 shows the first six mode shapes of this freely vibrating rectangular membrane, where m denotes the number of nodal lines parallel to the shorter sides of the rectangular membrane, and n denotes the number of nodal lines parallel to the longer sides. The first six modes correspond to $(m = 0, n = 0)$, $(m = 1, n = 0)$, $(m = 0, n = 1)$, $(m = 2, n = 0)$, $(m = 1, n = 1)$ and $(m = 2, n = 1)$. It is found that the smoothness of the mode shapes is excellent and this can validate the perfect accuracy of the LRBFDQ results for wavenumbers as presented in Table 2.

5.3. Half-circle+triangle membrane

As shown in the previous two cases, the two-dimensional domains of circular and rectangular shapes are usually regarded as simple geometries, and these problems can also be easily handled by using the traditional FDM and the differential quadrature method (DQM). However, if a problem domain is of an arbitrary shape and cannot be easily transformed into a rectangular shape, then this problem cannot be easily solved by using FDM or DQM. In such cases, the use of a mesh-free method becomes a better choice. In this sub-section, we use the example of the freely vibrating half-circle + triangle membrane to demonstrate the capability of the LRBFDQ method in solving problems with arbitrarily shaped domains. The geometry of this membrane is

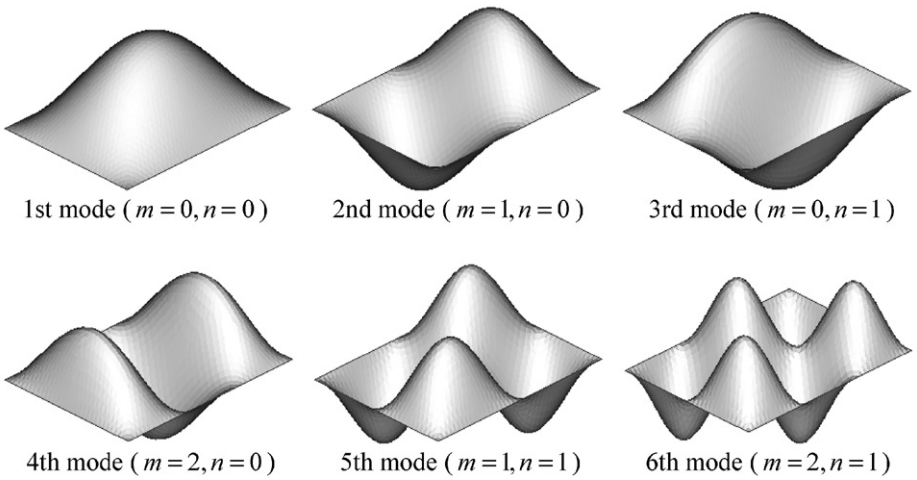

Fig. 9. Mode shapes of the rectangular membrane.

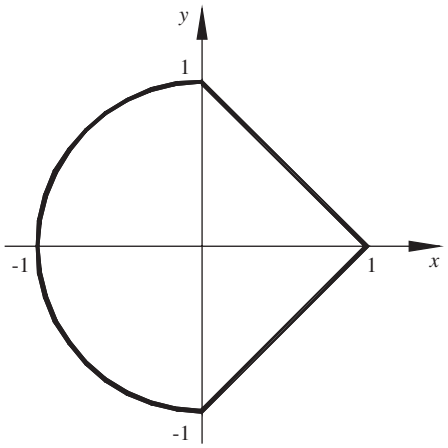

Fig. 10. Geometry of the half-circle + triangle membrane.

defined in Fig. 10. Table 3 shows the LRBFDQ results for the first eight wavenumbers that are computed by using three distributions of points in the domain, i.e. $N = 654$, 1048 and 1675. For this case, there are no exact solutions. Only the numerical solutions obtained by Kang et al. [7] using the non-dimensional dynamic influence function and 24 boundary points, and the FEM results using 1089 nodal points (Kang et al. [7]) are available for comparison. We can see that the LRBFDQ results are in very good agreement with Kang's numerical results, and it is observed that the LRBFDQ results are closer than FEM results to Kang's numerical results. Based on the comparison studies made in Tables 1 and 2 for the circular and rectangular membranes, it can be concluded that both the LRBFDQ results and Kang's numerical results are more accurate than FEM results for the half-circle + triangle membrane.

The mode shapes of the first six modes of this membrane are plotted in Fig. 11. The smoothness of these mode shapes is also excellent and this further confirms the high accuracy of the LRBFDQ results for the presented wavenumbers and mode shapes.

5.4. L-shaped membrane

The previous three cases are examples of vibrating membranes that have convex domain shapes. Usually, numerical problems with concave-shaped domains are more difficult to solve. In order to show the capability

Table 3
Comparison of wavenumbers of the half-circle + triangle membrane obtained by the present method, Kang et al. [7], and FEM [7]

Wavenumbers	LRBFDQ results			Kang [7]	FEM, $N = 1089$ [7]
	$N = 654$	$N = 1048$	$N = 1675$		
Λ_1	2.7104	2.7105	2.7106	2.7097	2.7230
Λ_2	4.2321	4.2320	4.2310	4.2279	4.2598
Λ_3	4.3578	4.3578	4.3579	4.3579	4.3786
Λ_4	5.5735	5.5730	5.5728	5.5649	5.6336
Λ_5	5.9341	5.9340	5.9339	5.9336	5.9846
Λ_6	6.1185	6.1182	6.1180	6.1159	6.1641
Λ_7	7.0148	7.0138	7.0134	6.9974	7.1334
Λ_8	7.1882	7.1881	7.1880	7.1868	7.3002

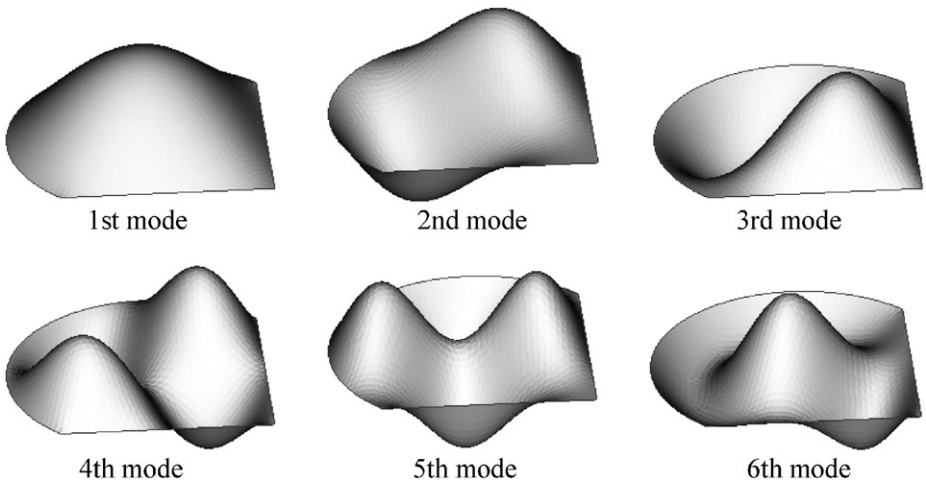

Fig. 11. Mode shapes of the half-circle + triangle membrane.

of the LRBFDQ method in solving problems with concave-shaped domains and yielding highly accurate solutions, we consider the L-shaped membrane. The geometry of this membrane is defined in Fig. 12. The LRBFDQ results for the first eight wavenumbers of this L-shaped membrane are obtained using three distributions of points in the domain, i.e. $N = 602$, 1018 and 1583 as shown in Table 4. The numerical results obtained by Kang and Lee [8] using the non-dimensional dynamic influence function and 28 boundary points, and FEM results using 1281 nodal points [8] are also displayed in Table 4 for comparison. The LRBFDQ results are found in good agreement with Kang's results and FEM results. It is noted that in Kang's approach, the concave domain must be divided into several convex sub-domains. This is because the trial functions used in Kang's approach are global functions that cannot approximate a function in a concave domain accurately. On the other hand, by using the LRBFDQ method, it is not necessary to use the domain decomposition technique because the LRBFDQ method makes use of local approximation.

Similar to previous cases, the accuracy of the LRBFDQ results for this L-shaped membrane is further confirmed by the observation of the high degree of smoothness of the first six mode shapes, as shown in Fig. 13.

5.5. Concave membrane with high concavity

Fig. 14 shows a concave shaped membrane with a high concavity due to the notch shaped cutout. Compared with the previous L-shaped membrane, the concavity of the domain shape of this membrane is considerably

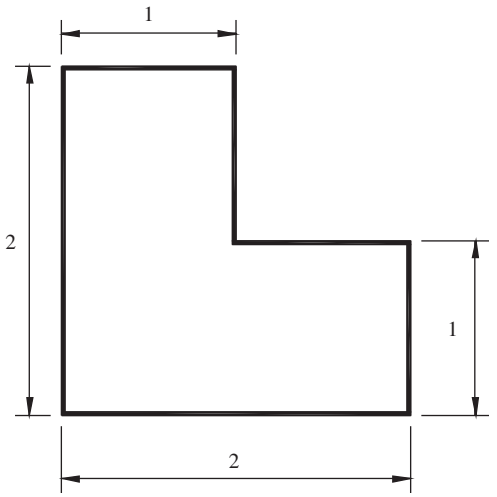

Fig. 12. Geometry of the L-shaped membrane.

Table 4
Comparison of wavenumbers of the L-shaped membrane obtained by the present method, Kang and Lee [8], and FEM [8]

Wavenumbers	LRBFDQ results			Kang [8]	FEM, $N = 1281$ [8]
	$N = 602$	$N = 1018$	$N = 1583$		
Λ_1	3.1159	3.1141	3.1124	3.14	3.11
Λ_2	3.8979	3.8981	3.8982	3.89	3.90
Λ_3	4.4429	4.4429	4.4429	4.44	4.45
Λ_4	5.4337	5.4334	5.4334	5.43	5.44
Λ_5	5.6644	5.6615	5.6593	5.70	5.67
Λ_6	6.4501	6.4484	6.4469	6.48	6.47
Λ_7	6.7037	6.7038	6.7039	6.69	6.73
Λ_8	7.0255	7.0251	7.0249	7.03	7.05

higher. Normally, higher concavity of problem domains may cause larger errors in numerical solutions. In order to investigate the capability of the LRBFDQ method in solving problems with high concavity in domain shapes, we choose the membrane shown in Fig. 14 as a numerical example. The LRBFDQ results for the first eight wavenumbers are computed by using three point distributions in the domain, i.e. $N = 514$, 1019 and 1591, and they are displayed in Table 5. The numerical results obtained by Kang and Lee [8] using the non-dimensional dynamic influence function and 30 boundary points, and the FEM results obtained using 1701 nodal points [8] are also listed in Table 5 for the purpose of comparison. The good agreement between the three results is evident. For the same reason as in the case of L-shaped membrane, this highly concave domain must be divided into two convex sub-domains so that Kang's approach can be applied, and obviously the division along the vertical centerline is the best choice. On the contrary, the domain decomposition technique is not needed when the LRBFDQ method is used to solve this problem. The high accuracy of the LRBFDQ results for this case is ensured by the properties of mesh-free and local approximation of the IQ-type RBF.

The evolvement of the mode shapes of this concavely shaped membrane is shown in Fig. 15. This evolvement is very interesting especially when compared with that of the rectangular membrane that has been discussed in the Section 5.2. As shown in Fig. 14, this concavely shaped membrane is modified from the rectangular membrane by restraining the deflections of membrane at the sharp V-shaped line-segments which are close to the vertical centerline. These additional restraints have obvious effects on the evolvement of the mode shapes. By observing and comparing the mode shapes as shown in Figs. 15 and 9, we can see that the

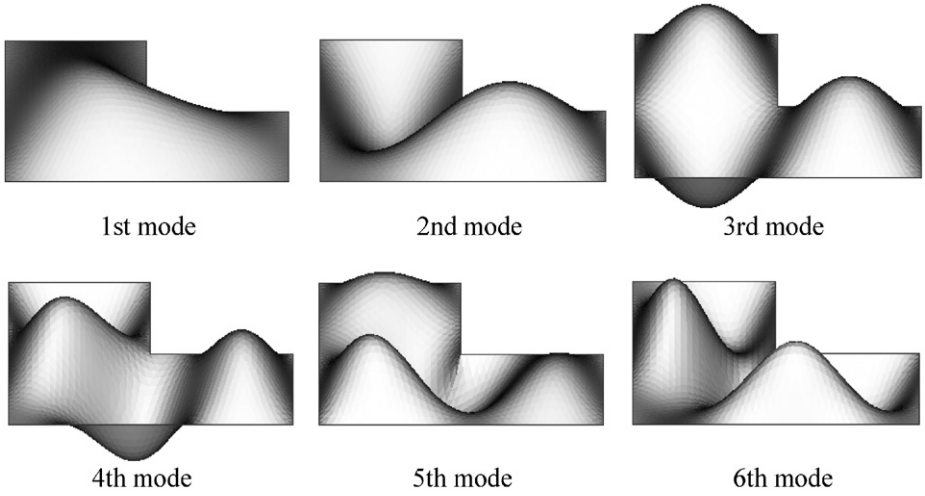

Fig. 13. Mode shapes of the L-shaped membrane.

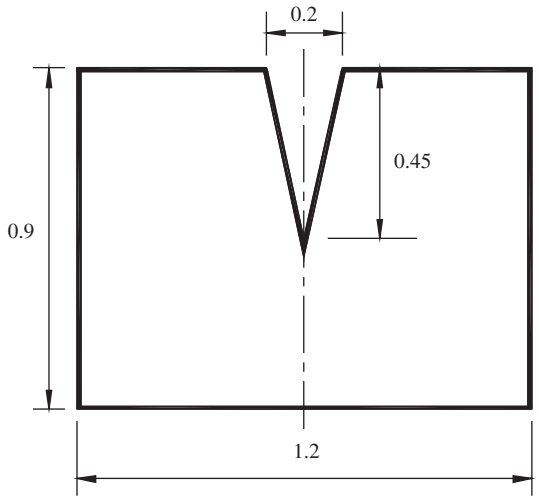

Fig. 14. Geometry of the concavely shaped membrane.

first three mode shapes of the concavely shaped membrane and the rectangular membrane have some relationships. That is, if zero deflection is enforced at the V-shaped line-segments of the rectangular membrane, the first three mode shapes of the rectangular membrane shown in Fig. 9 would have similar patterns of the first three mode shapes of the concavely shaped membrane shown in Fig. 15. From the rectangular membrane to the concavely shaped membrane, the change in the first mode shape is considerable. This is because the V-notch constraint of the concavely shaped membrane is applied in the large deflection region of the rectangular membrane. Similarly, the change in the third mode shape between the two membranes is also considerable. On the other hand, the change in the second mode shape is not obvious. This is because the additional restraints at the V-shaped line-segments are close to the original nodal line of the second mode shape of the rectangular membrane. Furthermore, the fourth mode shape of the concavely shaped membrane corresponds to the fifth mode shape of the rectangular membrane. The difference between them is also minor because the V-shaped line-segments on the boundary of the concavely shaped membrane are close to one nodal line of the fifth mode shape of the rectangular membrane. It is noted that the wavenumbers of the second and fourth modes of the concavely shaped membrane are slightly higher than the

Table 5
Comparison of wavenumbers of the concavely shaped membrane obtained by the present method, Kang and Lee [8], and FEM [8]

Wavenumbers	LRBFDQ results			Kang [8]	FEM, $N = 1701$ [8]
	$N = 514$	$N = 1019$	$N = 1591$		
Λ_1	5.7789	5.7253	5.7470	5.79	5.71
Λ_2	6.4187	6.4190	6.4186	6.42	6.42
Λ_3	8.1817	8.1679	8.1733	8.15	8.17
Λ_4	8.8845	8.8852	8.8845	8.88	8.89
Λ_5	9.8961	9.8608	9.8757	9.92	9.87
Λ_6	11.2604	11.2629	11.2627	11.25	11.31
Λ_7	11.4664	11.4364	11.4503	11.55	11.46
Λ_8	11.8153	11.8180	11.8172	11.81	11.84

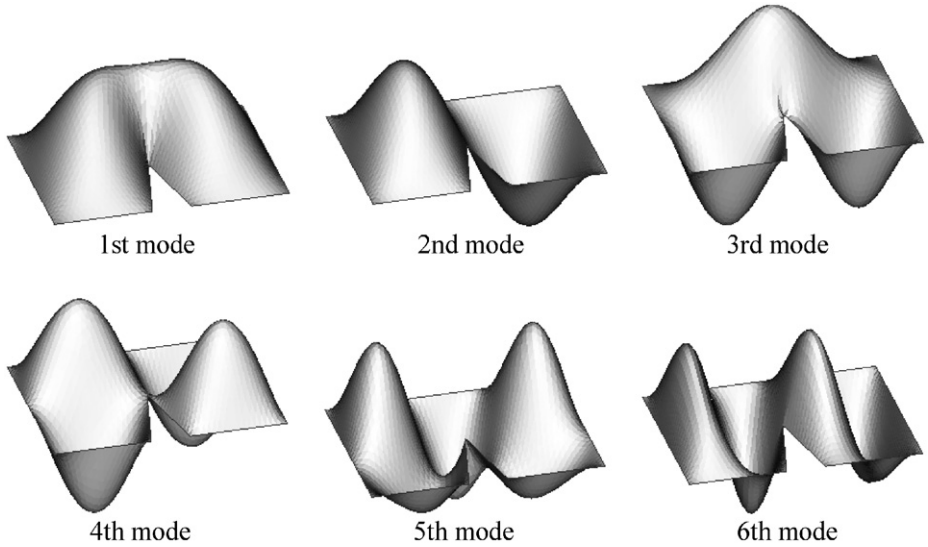

Fig. 15. Mode shapes of the concavely shaped membrane.

wavenumbers of the second and fifth modes of the rectangular membrane, respectively. This is related to the similarities between their mode shapes. Finally, it can be expected that the fifth and sixth mode shapes of the concavely shaped membrane should correspond to two mode shapes of the rectangular membrane that are not shown in Fig. 9.

5.6. *Multi-connected membrane*

In this last numerical example, a multi-connected membrane as defined in Fig. 16 is considered. This domain shape can be regarded as the most complex one among the domain shapes in this study because it is not only concave but also multi-connected. Successful computation of this case will demonstrate the power of the LRBFDQ method. Table 6 shows the LRBFDQ results for the first ten wavenumbers of this multi-connected membrane computed by using three point distributions in the domain, i.e. $N = 733$, 1274 and 1800. The convergence behavior of these solutions is evident. The numerical solutions obtained by Kang and Lee [8] using the non-dimensional dynamic influence function and 52 boundary points, and FEM solutions using 880 nodal points [8] are also listed in Table 6 for the purpose of comparison. It is found that the LRBFDQ results agree well with Kang's results and FEM results. It should be noted that, by using Kang's approach, the multi-connected domain must be divided into four convex sub-domains, and the dividing lines coincide with the

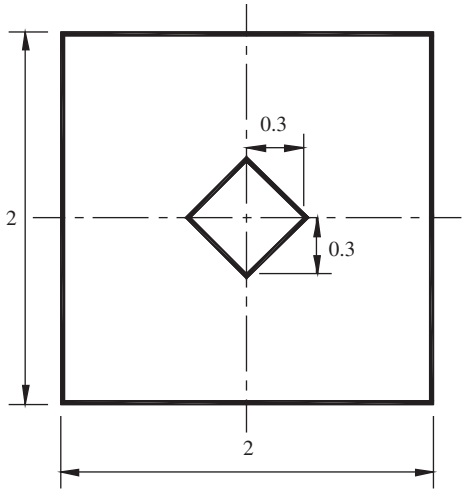

Fig. 16. Geometry of the multi-connected membrane.

Table 6
Comparison of wavenumbers of the multi-connected membrane obtained by the present method, Kang and Lee [8], and FEM [8]

Wavenumbers	LRBFDQ results			Kang [8]	FEM, $N = 880$ [8]
	$N = 733$	$N = 1274$	$N = 1800$		
Λ_1	3.7039	3.6808	3.6731	3.71	3.67
Λ_2	4.0027	3.9854	3.9800	4.00	3.99
Λ_3	4.5063	4.5080	4.5084	4.50	4.53
Λ_4	5.2226	5.2023	5.1964	5.27	5.19
Λ_5	5.8779	5.8651	5.8615	5.90	5.89
Λ_6	6.4578	6.4401	6.4344	6.48	6.51
Λ_7	7.0289	7.0287	7.0287	7.03	7.07
Λ_8	7.1258	7.1188	7.1156	7.12	7.24
Λ_9	7.2403	7.2444	7.2455	7.23	7.39
Λ_{10}	7.7347	7.7251	7.7211	7.77	7.73

vertical and horizontal centerlines. The domain decomposition technique is not necessary for the LRBFDQ method because of its local approximation and mesh-free properties.

Similar to previous cases, the good accuracy of LRBFDQ solutions of this multi-connected membrane is further confirmed by the satisfactory smoothness of the mode shapes, the first six of which are plotted in Fig. 17.

6. Conclusions

The LRBFDQ method has been successfully applied to compute wavenumbers and mode shapes of vibrating membranes with arbitrary domain shapes. The LRBFDQ method was developed from the global RBF-based interpolation method. The features of the LRBFDQ method that are inherited from the global RBF-based interpolation method include: (1) using RBFs as base functions to interpolate function value or to approximate derivatives; (2) nature of mesh-free. These two features ensure that high accuracy of interpolation and approximation is kept, and the method is suitable for problems with arbitrary domain shapes. The new features of the LRBFDQ method include: (1) interpolation of function value and approximation of derivatives are made in local regions; (2) coefficients in the local approximation to derivatives can be easily determined by using analysis of a linear vector space. These two features ensure that the resultant algebraic equation systems

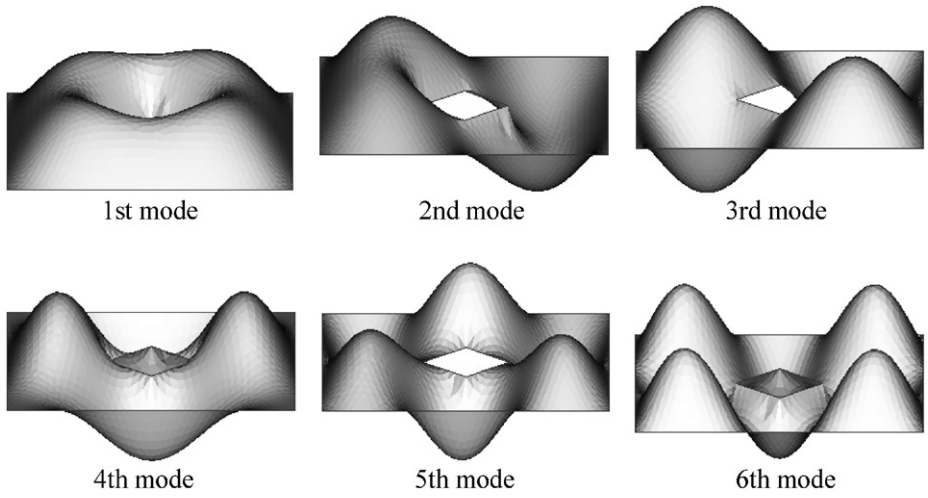

Fig. 17. Mode shapes of the multi-connected membrane.

of large-scale problems are solvable, and the process of discretization of differential equations becomes very simple.

In the LRBFDQ method, the number of supporting points in the local supporting region of each reference point, m, the shape parameter, c, and the average distance between neighboring points, h, are three major factors that affect the accuracy and stability of numerical solutions. This is revealed by solving the sample Poisson equation. It is found that, when IQ is chosen as the RBF, the choices of $m \approx 16$ and $0.6 \leqslant c \leqslant 1.5$ can ensure both accuracy and stability of solutions. For all the membrane shapes considered herein, the use of the LRBFDQ scheme with IQ as the RBF, $m = 16$ as the number of supporting points of each reference point, and $c = 1.0$ as the value of shape parameter yields very accurate solutions. Accurate computation of the wavenumbers and mode shapes of several membranes with typical domain shapes demonstrates the applicability of the LRBFDQ method for solving PDEs with arbitrarily shaped domains.

References

[1] H.D. Conway, K.A. Farnham, The free flexural vibrations of triangular, rhombic and parallelogram plates and some analogies, *International Journal of Mechanical Sciences* 7 (1965) 811–816.
[2] S. Durvasula, Natural frequencies and modes of skew membranes, *The Journal of the Acoustical Society of America* 44 (1968) 1636–1646.
[3] L. Bauer, E.L. Reiss, Free vibrations of rhombic plates and membranes, *The Journal of the Acoustical Society of America* 54 (1973) 1373–1375.
[4] T. Irie, G. Yamada, K. Umesato, Free vibration of regular polygonal plates with simply supported edges, *The Journal of the Acoustical Society of America* 69 (1981) 1330–1336.
[5] T. Irie, G. Yamada, M. Tsujino, Natural frequencies of concavely shaped polygonal plates with simply supported edges, *The Journal of the Acoustical Society of America* 69 (1981) 1507–1509.
[6] A.W. Leissa, *Vibration of Plates*, Acoustical Society of America, 1993.
[7] S.W. Kang, J.M. Lee, Y.J. Kang, Vibration analysis of arbitrarily shaped membranes using non-dimensional dynamic influence function, *Journal of Sound and Vibration* 221 (1999) 117–132.
[8] S.W. Kang, J.M. Lee, Application of free vibration analysis of membranes using the non-dimensional dynamic influence function, *Journal of Sound and Vibration* 234 (2000) 455–470.
[9] J.W. Strutt, B. Rayleigh, *The Theory of Sound*, second ed., Dover Publications, New York, 1945.
[10] L.E. Kinsler, A.R. Frey, A.B. Coppens, J.V. Sanders, *Fundamentals of Acoustics*, third ed., Wiley, New York, 1982.
[11] N.W. McLachlan, Vibrational problems in elliptical coordinates, *Quarterly of Applied Mathematics* 5 (1947) 289–297.
[12] C. Shu, H. Ding, K.S. Yeo, Local radial basis function-based differential quadrature method and its application to solve two-dimensional incompressible Navier–Stokes equations, *Computer Methods in Applied Mechanics and Engineering* 192 (2003) 941–954.
[13] R.E. Bellman, B.G. Kashef, J. Casti, Differential quadrature: a technique for the rapid solution of nonlinear partial differential equations, *Journal of Computatonal Physics* 10 (1972) 40–52.
[14] C. Shu, *Differential Quadrature and its Application in Engineering*, Springer, London, 2000.

[15] C. Shu, B.E. Richards, Application of generalized differential quadrature to solve two-dimensional incompressible Navier–Stokes equations, *International Journal for Numerical Methods in Fluids* 15 (1992) 791–798.
[16] P. Malekzadeh, G. Karami, M. Farid, DQEM for free vibration analysis of Timoshenko beams on elastic foundations, *Computational Mechanics* 31 (2003) 219–228.
[17] P. Malekzadeh, G. Karami, M. Farid, A semi-analytical DQEM for free vibration analysis of thick plates with two opposite edges simply supported, *Computer Methods in Applied Mechanics and Engineering* 193 (2004) 4781–4796.
[18] G. Karami, P. Malekzadeh, In-plane free vibration analysis of circular arches with varying cross-sections using differential quadrature method, *Journal of Sound and Vibration* 274 (2004) 777–799.
[19] P. Malekzadeh, G. Karami, Vibration of non-uniform thick plates on elastic foundation by differential quadrature method, *Engineering Structures* 26 (2004) 1473–1482.
[20] P. Malekzadeh, G. Karami, Polynomial and harmonic differential quadrature methods for free vibration of variable thickness thick skew plates, *Engineering Structures* 27 (2005) 1563–1574.
[21] G. Karami, P. Malekzadeh, An efficient differential quadrature methodology for free vibration analysis of arbitrary straight-sided quadrilateral thin plates, *Journal of Sound and Vibration* 263 (2003) 415–442.
[22] C.W. Bert, M. Malik, The differential quadrature method for irregular domains and application to plate vibration, *International Journal of Mechanical Sciences* 38 (1997) 589–606.
[23] E.J. Kansa, Multiquadrics—a scattered data approximation scheme with applications to computational fluid-dynamics—I. Surface approximations and partial derivative estimates, *Computers and Mathematics with Applications* 19 (1990) 127–145.
[24] E.J. Kansa, Multiquadrics—a scattered data approximation scheme with applications to computational fluid-dynamics—II. Solutions to parabolic, hyperbolic and elliptic partial differential equations, *Computers and Mathematics with Applications* 19 (1990) 147–161.
[25] W.H. Press, B.P. Flannery, S.A. Teukolsky, W.T. Vetterling, *Numerical Recipes in Fortran 77: The Art of Scientific Computing*, Cambridge University Press, London, 1993.